END
DATE
FILMED

12-84

DTIC

MICROCOPY RESOLUTION TEST CHART

AD-A147 581

AFGL-TR-84-0143

RESEARCH IN GEODESY BASED UPON RADIO
INTERFEROMETRIC OBSERVATIONS OF
EXTRAGALACTIC RADIO SOURCES

T.A. Herring
J.L. Davis
I.I. Shapiro

Harvard College Observatory
60 Garden Street
Cambridge, Massachusetts 02138

May 1984

Scientific Report No. 1

DTIC
ELECTE
NOV 1 6 1984
B

AIR FORCE GEOPHYSICS LABORATORY
AIR FORCE SYSTEMS COMMAND
UNITED STATES AIR FORCE
HANSCOM AFB, MASSACHUSETTS 01731

84   11   06   05 8

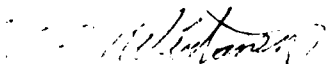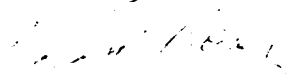CONTRACTOR REPORTS

This technical report has been reviewed and is approved for publication.

THEODORE E. WIRTANEN
Contract Manager

THOMAS P. ROONEY
Chief, Geodesy & Gravity Branch

FOR THE COMMANDER

DONALD H. ECKHARDT
Director
Earth Sciences Division

AD A147581

REPORT DOCUMENTATION PAGE

1a. REPORT SECURITY CLASSIFICATION	1b. RESTRICTIVE MARKINGS
Unclassified	

2a. SECURITY CLASSIFICATION AUTHORITY	3. DISTRIBUTION/AVAILABILITY OF REPORT
	Approved for public release;
2b. DECLASSIFICATION/DOWNGRADING SCHEDULE	distribution unlimited

4. PERFORMING ORGANIZATION REPORT NUMBER(S)	5. MONITORING ORGANIZATION REPORT NUMBER(S)
	AFGL-TR-84-0143

6a. NAME OF PERFORMING ORGANIZATION	6b. OFFICE SYMBOL (If applicable)	7a. NAME OF MONITORING ORGANIZATION
Harvard University Harvard College Observatory		

6c. ADDRESS (City, State and ZIP Code)	7b. ADDRESS (City, State and ZIP Code)
60 Garden Street Cambridge, MA 02138	

8a. NAME OF FUNDING/SPONSORING ORGANIZATION	8b. OFFICE SYMBOL (If applicable)	9. PROCUREMENT INSTRUMENT IDENTIFICATION NUMBER
Air Force Geophysics Laboratory	LWG	F19628-83-K-0031

8c. ADDRESS (City, State and ZIP Code)	10. SOURCE OF FUNDING NOS.			
Hanscom AFB, MA 01731 Monitor/Theodore E. Wirtanen	PROGRAM ELEMENT NO.	PROJECT NO.	TASK NO.	WORK UNIT NO.
	61102F	2309	G1	BE

11. TITLE (Include Security Classification) RESEARCH IN GEODESY BASED UPON RADIO INTERFEROMETRIC OBSERVATIONS OF EXTRAGALACTIC RADIO SOURCES

12. PERSONAL AUTHOR(S)
Herring, T.A., Davis, J.L., and Shapiro, I.I.

13a. TYPE OF REPORT	13b. TIME COVERED	14. DATE OF REPORT (Yr., Mo., Day)	15. PAGE COUNT
Scientific Report No 1	FROM 3/17/83 TO 3/16/84	84/5	40

16. SUPPLEMENTARY NOTATION

17.	COSATI CODES		18. SUBJECT TERMS (Continue on reverse if necessary and identify by block number)
FIELD	GROUP	SUB. GR.	Radio Interferometry, Geodesy, Intercontinental Distance Measurement

19. ABSTRACT (Continue on reverse if necessary and identify by block number)

See reverse side for abstract.

20. DISTRIBUTION/AVAILABILITY OF ABSTRACT	21. ABSTRACT SECURITY CLASSIFICATION
UNCLASSIFIED/UNLIMITED ☐ SAME AS RPT. ☐ DTIC USERS ☐	

22a. NAME OF RESPONSIBLE INDIVIDUAL	22b. TELEPHONE NUMBER (Include Area Code)	22c. OFFICE SYMBOL

DD FORM 1473, 83 APR   EDITION OF 1 JAN 73 IS OBSOLETE.

19. Abstract

Very-long-baseline interferometric (VLBI) observations obtained from a network of radio telescopes distributed in North America and Europe have been analyzed to estimate the relative positions of the radio telescopes and the nutations of the Earth's rotation axis. In addition to the estimation of these geodetic parameters we have also used some of these data to study the Mark III instrumental performance, and the calibration of the atmospheric delay.

The analysis of the Mark III instrumentation has allowed us to isolate the probable cause of S-band group delay closure errors. These closure errors appear to be due to the effects of the "leakage" of left-circularly polarized radiation into the output of feed horns which are designed to receive only right-circularly polarized radiation. This instrumental error appears to have affected the ionospheric-calibrated group delays at the 1 cm level.

The investigations of the effects of the atmospheric delay calibration on the estimates of geodetic parameters have disclosed that the elevation angle dependence of the dry atmospheric delay model (Marini model) may be biased. We suspect that this delay model may be biased by about 10 cm at $10°$ elevation angle. A bias of this magnitude is not unlikely because two models of the elevation angle dependence of the atmospheric delay (Chao and Marini) differ by about 6 cm at $10°$ elevation angle.

The estimates of the baseline length between our two primary antennas (Westford Observatory in North America, and Onsala Space Observatory in Europe), show an apparent rate of change of 1.6 ± 0.5 cm/yr, with a weighted-root-mean-square (WRMS) scatter of the individual length estimates about the best fit straight line of 2.0 cm. Even though the estimated rate of change is over three standard deviations we do not claim to have detected the relative motions of the North American and Eurasian tectonic plates because we feel that systematic errors (mainly due to the atmospheric delay calibration) could affect our baseline length estimates by an amount equal to the apparent change in the length over the three year span of our data.

We have also made estimates of the errors in the nutation series based on our geodetic experiments. We see a significant error in the annual retrograde nutation amplitude of -1.9 ± 0.2 mas, in phase, and 0.8 ± 0.2, out of phase. We believe that these errors in the nutation series are due to an error of approximately 1/30 cycles/sidereal day in the frequency of the resonance in the Earth's rotational motion due to the fluid core. This error in the frequency is the same magnitude as the error in the frequency of the Chandler wobble which is calculated from the same formalism used to compute the core resonance frequency. It is not yet clear that the origin of the errors in these two frequencies are related.

Accession For
NTIS GRA&I
DTIC TAB
Unannounced
Justification

By
Distribution/
Availability Codes
Avail and/or
Dist   Special

A-1

DTIC
ELECTE
NOV 1 6 1984
B

1. Significant Accomplishments

Under this contract we have been examining many facets of the geodetic very-long-baseline interferometric technique ranging from instrumental performance to the geophysical implications of the results thus far obtained with this system. This section will be divided into four subsections in which we discuss significant results obtained during the past twelve months.

1.1 Instrumental Errors

We have continued to monitor the quality of the Mark III group delay measurements by comparing the group- and phase-delay measurements. In the past these comparisons have allowed us to detect the presence of spurious signals in the Mark III system which introduced errors in the group delays of up to 3 cm. The continued examination of the group- and phase-delay measurements have allowed us, in conjunction with A.E.E. Rogers at the Haystack Observatory, to isolate the cause of a problem which has been evident for a number of years. Since the July 1980 experiment, it has been clear that the S-band (2.3 GHz) group delay closures (i.e., the sum of the delays around a triplet of baselines), were biased by up to 0.4 nsec (12 cm equivalent path delay). These closure errors would introduce errors in the ionospheric-calibrated group delays of approximately 1 cm. The cause of these closure biases

-4-

is now thought to be due to the effects of feed horn imperfections. The imperfections in the feed horns allow left-circularly polarized (LCP) radiation to "leak" into the output of the nominally right-circularly polarized (RCP) feed horns.

In Figure 1.1.1 we show the S-band group delay closure errors for the Haystack-Onsala-Effelsberg baseline triplet during a six hour span of data from the July 1980 experiment. The solid curve in this figure is the expected contribution of the feed polarization error.

The feed polarization error will also affect the prediction of the phase delay ambiguities from the group-delay measurements. In Figure 1.1.2 we show the differences between the group delay measurements from a 12 hour section of the December 1982 experiment and estimates of their values computed from the phase delays. The curve superimposed on this figure is the expected contribution of the feed polarization error.

We are currently developing software which will allow us to examine more experiments for this effect and to analyze any time dependence of the feed horn parameters. Steps are also being undertaken to better isolate the LCP and the RCP outputs so that this error will not be a problem in the future.

1.2 WVR Data Analysis and Calibration of the Troposphere

Early in 1983 we were able to correct a deficiency in the

then-current WVR processing algorithms. The deficiency was caused by the random noise introduced into the estimates of the WVR's internal gain by the extrapolation of the power output at the temperature of the two calibration loads (maintained at roughly 300 K and 400 K) down to the power output at the temperature of the atmosphere (usually < 100 K). This resulted in estimates of the zenith delay which displayed a short term scatter of approximately 1 cm. Furthermore, it is now believed that uncorrected drifts in the so-called "hot load correction" on time scales of several hours were causing systematic drifts of the estimated zenith delay from the true zenith delay of as much as 1-2 cm. (The hot load correction is an additive term to correct the physical temperature of the hotter calibration load, which can be different from the effective temperature of that load due to reflections and losses occurring principally at the switch placed between the calibration loads and the WVR antenna. It is typically less than 10 K in magnitude.) We found that estimation of the gain by frequent tip curves provided more precise estimates of the WVR gain; this gain inherently included the actual hot load correction at the time the tip curve was performed. The resulting estimates of the zenith delay were found to have a reduced short-term scatter (~ 3 mm) and are believed to have much smaller systematic drifts arising from instrumental variations.

We also began using the estimates of the wet delay determined by this new method to correct VLBI group-delay observations. To

date, there are only six observing sessions, each for a duration
of roughly one day, for which there exist WVR data, obtained from
tip curves, with working WVR's being stationed at at least three
of the VLBI sites participating in that observing session. Four
of these observing sessions are from the four days from 15 to 18
December 1982. During these sessions there were WVR's at Ft. Davis,
Owens Valley, and Onsala. For the 6 May 1983 observing session
there were operational WVR's at Westford, Ft. Davis, and Onsala,
and on 23 August 1983 there were operational WVR's at Mojave, Ft.
Davis, and Owens Valley. It was originally hoped that a comparison
of baseline solutions utilizing different wet delay correction
techniques would provide evidence as to whether the WVR was indeed
capable of correcting much of the short term scatter of the VLBI
postfit residuals. However, the effect which was found to dominate
the comparison was a systematic difference of the estimated baseline
lengths produced by solutions with and without daily corrections
to the overall zenith delay being estimated for each site.

Figure 1.2 contains a plot of this effect as a function of
baseline length. The weighted mean of the differences between the
estimate of the baseline length from solutions with a zenith delay
correction estimated and the estimates of the baseline length
without a zenith delay correction is plotted vertically. The
estimates of the site components used to generate the differences
have been obtained from group delays that have had the wet troposphere
calibrated with WVR data. It can be seen that the size of the

effect increases with increasing baseline length. Further analysis
of the solutions led us to the conclusion that the differences in
baseline length were due almost entirely to differences in the
estimated position of each of the antennas in the direction of the
respective local vertical. Since these differences were triggered
by the inclusion (or exclusion) of the zenith delay correction
parameter in the baseline solution, and since errors in the estimate
of this parameter are known to be highly correlated with estimates
of the site position in the direction of the local vertical, we
believed that the differences resulted from errors in the estimates
of the average zenith delay due to the "dry" component of the
atmosphere. The estimate of the dry term is obtained from any one
of several available models parameterized by surface weather
conditions. What was not understood is why the error in the dry
term should be of a systematic nature, given that the experiments
took place under much different seasonal conditions (Winter, Spring,
and Summer), and the various sites used are located in extremely
different climates (Northeast U.S., Southwest U.S., Southern Sweden).

We now believe that the effect is caused by an error in the
"mapping function," the expression which relates the delay in the
zenith direction to the delay in the direction of observation (at
elevation e). If the earth were flat, its atmosphere homogeneous
and isotropic, and if the effects of refraction were ignored, then
the mapping function would be given simply by the cosecant of the
elevation. The largest errors in the cosecant law are caused by

the first and final of the above assumptions; the errors due to
the assumptions of homogeneity and isotropism are primarily
statistical in nature. It has been found convenient to parameterize
the mapping function crudely as

$$m(e;a) = [\sin(e) + a]^{-1}, \quad a \geq 0$$

where we recover the cosecant law for a = 0. Using this formulation
of the mapping function, we can estimate the effect on the estimate
of the radial component of the site vector due to an error
$\Delta a = a_{assumed} - a_{true}$. Then, if the differences plotted in Figure
1.2 are due only to this error, we may usefully estimate it. (Also,
an assumption has been made that the total zenith delay is a
constant, independent of site. In fact, the total zenith delay
changes < 5% daily, and no more than 10% annually, for a particular
site. However, there can be a somewhat larger site dependence.)
Table 1.2 shows the implied values of Δa for a zenith delay of
230 cm. The weighted mean of the values for all the baselines is
$\Delta a = (1.1 \pm 0.2) \times 10^{-3}$. The relationship between the difference
in baseline length estimates Δb (cm) from solutions with and without
a zenith delay estimated, implied by this value for Δa, can be
written

$$\Delta b = (1.24 \pm 0.18) \times 10^{-3} \, B \, (cm/km)$$

where $\underline{B}$ (km) is the baseline length. The line representing this relationship is superimposed on Figure 1.2. It can be seen that this simple model is relatively successful in predicting the behavior of the differences as a function of baseline length. We hope to begin a more careful study of the elevation dependence of the tropospheric delay shortly.

We feel that there is evidence that the WVR does help reduce the scatter of the postfit residuals, although we cannot be certain of this due to the mapping function problem. Ultimately, when the mapping function problem is solved, we expect that the use of the WVR will obviate the need for the inclusion of the zenith delay correction parameter in the baseline solution. This parameter, as explained above, is highly correlated with station position, and its inclusion tends to increase the formal estimates of the standard deviations of the parameters by a factor of two. This effect would exist even after the mapping function had been corrected.

1.3 Baseline Length Analysis

We have been analyzing the baseline length results from a VLBI data set which contains approximately 32,000 group delay measurements obtained from 122 observing sessions, each of about 24 hours duration, carried out between July 1980 and June 1983. We have repeated the analysis of the data set a number of times using subsets of the data and using different atmospheric delay calibrations.

The aim of these studies is to gain a better understanding of the effects of systematic errors on the VLBI baseline length estimates. Since we believe that the atmospheric delay calibration is the major error source for VLBI, we have carried out tests which we believed would highlight the effects of atmospheric delay calibration errors.

Errors in the atmospheric delay calibration would be expected to show an elevation angle dependence and, hence, we have carried out a number of solutions in which we excluded from the analysis observations whose elevations are less than a specified limit called the "elevation angle cutoff." The changes in the baseline lengths when the elevation angle cutoff is changed are shown in Figures 1.3.1 (a)-(c). (The error bars in these figures are the expected standard deviations of the differences of the baseline length estimates because of the inclusion of additional data in solutions with lower elevation angle cutoffs.) From these figures we see that the baseline length estimates systematically depend on the minimum elevation angle of observations included in the data set. We currently believe that these systematic decreases of baseline length with increasing elevation angle cutoff are due to an error in the atmospheric mapping function, as explained in Section 1.2.

We further studied the dependence of the baseline length estimates on the atmospheric delay calibration by removing the Marini surface model atmospheric delay calibration and estimating the atmospheric delay solely from the VLBI data. (Even with the

surface model calibration, we estimated a zenith delay correction to account for any biases in the calibration of the atmospheric delay due to water vapor, as described in Section 1.2.) The changes of the baseline length estimates from these two types of solutions are shown in Figure 1.3.2. Again, we see a systematic change in the estimates of the baseline lengths; again, these changes are most probably due to the differences in the mapping functions for the Chao and Marini models. (The Chao mapping function is chosen as the mapping function for the zenith delay correction rather than the Marini mapping function because the Chao mapping function is independent of surface weather conditions and is simpler to calculate.) For typical atmospheric conditions, the difference in the mapping function for these two models can change the atmospheric delay calibration by 5 cm at a 10° elevation angle.

Thus far we have discussed the baseline length estimates from the analysis of the complete data set; we have also been studying the baseline length estimates from the individual 24 hour observing sessions. In Table 3.1, we show the estimates of the baseline lengths which were obtained from the 10° elevation angle cutoff solution with the Marini surface model atmospheric delay calibration. We also give the weighted-root-mean-square (WRMS) scatter of the length estimates from the analysis of the individual observing sessions (analyzed with the source positions constrained to the values obtained from the analysis of the complete data set). We also present the WRMS scatter of the baseline length estimates from

the solutions with a 0° elevation cutoff angle. We note that in almost all cases the WRMS scatter of the length estimates from the solutions with the lower elevation angle cutoff are less than those from solutions with the low elevation angle observations excluded. This result is even more surprising when we realize that the number of observations with elevation angles less than 10° constitute only 2% of the total data set. These results would indicate that the deviations between the atmospheric delay and the model of this delay for elevation angles less than 10° are not as large as previously had been suspected.

The repeatability of the Westford, MA to Onsala, Sweden baseline is of most interest to us because it is this baseline which will probably yield or place a useful upper bound on the contemporary rate of motion of the North American and Eurasian tectonic plates. We show the time history of the baseline length estimates between these two locations in Figure 1.3.3. For experiments prior to May 1981, the Haystack Observatory in Massachusetts, rather than the Westford Observatory, was used and we have inferred the Westford-to-Onsala baseline length from the relative position of these two radio telescopes (1.24 km apart) determined from the Mark I VLBI short baseline experiments (see discussions later in this section). The estimate of the rate of change of the Westford-to-Onsala baseline is 1.6 ± 0.5 cm/yr. The rate uncertainty is calculated by multiplying the statistical estimate of the standard deviation of the rate estimate by the ratio of the scatter of the estimates about their

mean to the expected scatter given by the standard deviations of the individual estimates. This ratio is called the normalized-root-mean-square (NRMS) scatter. Although the rate estimate is over three standard deviations, we do not yet claim to have detected the relative motions of these two sites because we feel that over the three year period spanned by the data set, the change in the length (4.8 cm) has not yet exceeded the changes which could be caused by the effects of systematic errors (mainly the atmospheric delay).

We mentioned earlier in this section that the Westford-to-Onsala baseline length results are composed of experiments which used two radio telescopes in Massachusetts: Haystack Observatory and Westford Observatory. In order to combine these two sets of results without introducing a large offset, we need an accurate estimate of the relative positions of the two antennas. (The antennas are separated by 1.24 km, which is sufficiently small that errors in the BIH pole position and AT-UT1 will introduce errors of less than 1 mm in the relative coordinates of the antennas.) In order to confirm the estimates of relative positions of these two antennas, we have analyzed the phase delay data from the Mark III experiments which simultaneously involved these two antennas. (The original estimates of the relative positions were obtained from Mark I VLBI experiments.) There are seven Mark III experiments which can be used to determine the relative positions. The results of the analysis of these experiments are shown in Table 1.3.2. These results are also shown

in graphical form in Figures 1.3.4 (a) and (b). The WRMS scatter of the (locally) horizontal coordinates of the Westford antenna relative to the Haystack antenna is 1.0 mm in both the North-South and East-West components. The WRMS scatter of the vertical component is 4.4 mm. The difference between the Mark III results and the Mark I results will change the inferred Westford-to-Onsala baseline lengths (from experiments which involved the Haystack Observatory) by only 1 mm. This change is small compared to the 20 mm WRMS scatter of the Westford-to-Onsala baseline length estimates.

The Mark III Haystack-to-Westford short-baseline results represent the best VLBI baseline measurements to date. They also imply (at least for these two antennas) that the structural stability of the radio telescopes should pose no major problems to the detection of crustal movements using VLBI.

1.4 Nutations of the Earth's Rotation Axis

In this final part of the significant accomplishments section we turn our attention to some tentative geophysical results which have been obtained with VLBI. Observations of extragalactic radio sources provide the best approximation to an inertial reference frame which is observationally possible at this time. We have been using this capability of VLBI to study the nutations of the Earth's rotation axis. (Strictly, the observed nutations are not referred to the rotation axis but rather to an axis which would be fixed to

the mean outer surface of the Earth, if the Earth were not undergoing free motion, i.e., polar motion. The observed axis will be referred to as the "body axis.") The method we have adopted to study the nutations is to estimate from each 24 hour VLBI experiment a correction to the nutations in latitude ($\Delta\epsilon$) and longitude ($\Delta\psi$) as given by the Wahr nutation series (Wahr, 1981). Corrections to the Wahr nutation series coefficients are then calculated by estimating the amplitudes of the periodic components in the time series of $\Delta\epsilon$ and $\Delta\psi$ as given by the arguments of the nutation series. We also estimate the amplitudes of the periodic terms which are $90°$ out of phase with the nutation series arguments. These terms, referred to as the "out of phase" components, are related to the energy dissipation occurring in the Earth. In Figures 1.4.1(a) and (b) we present the estimates of the corrections to $\Delta\epsilon$ and $\Delta\psi\sin\epsilon_o$ for each of the 122 experiments which we have been analyzing. Table 4.1 gives the estimates of the corrections to the Wahr nutation series coefficients and the out of phase components which are implicitly zero in the (dissipationless) Wahr nutation series.

Of the six frequency components estimated only the annual and the semi-annual components have corrections which are greater than three standard deviations. (The estimates of the standard deviations were obtained by scaling the statistical estimates from the weighted-least squares solutions by the NRMS scatter of the residual nutation angles. The scaling factors for both $\Delta\epsilon$ and $\Delta\psi\sin\epsilon_o$ were

2.0. This capability of assessing the quality of the estimates of the nutation angles is one of the advantages of estimating the nutation angle corrections rather than directly estimating the corrections to the series coefficients.)

The nutation angles $\Delta\epsilon$ and $\Delta\psi$ are convenient angles to use for coordinate system rotations. However, for the geophysical interpretation of these results it is more convenient to analyze the amplitudes of the circular nutations. Each tidal constituent will produce a forced response of the Earth's rotation at its frequency, with only the nearly diurnal frequencies producing a measurable response. On the rotating Earth these frequencies will appear as nearly diurnal and in inertial space they will appear as long period motions of the rotation axis, i.e. nutations. Each pair of tidal frequencies which are symmetric about one sidereal day will generate nutations with the same absolute frequency (when viewed from inertial space), but with one rotating in the same sense as the Earth (the prograde term) and the other rotating with the opposite sense (the retrograde term). The prograde and retrograde nutation amplitudes when normalized by the tidal amplitude at their frequency give the response of the Earth to a forced motion. In Table 1.4.2 we give the estimates of the corrections to the nutation amplitudes for each of the nutation frequencies given in Table 1.4.1. From Table 1.4.1 we see that only the prograde semiannual and the retrograde annual terms have significant corrections (greater than 3 sigma).

The Wahr nutation series, while being the most complete treatment of the forced response of the Earth available at this time, does not fully model the actual properties of the Earth. It is already known that the oceans will affect the response of the Earth. This effect has been estimated by Wahr and Sasao (1981) and is summarized in Table 1.4.3. The effects of the oceans match the observed error in the prograde semiannual term. However, the ocean effects do not explain the large error in the retrograde annual term.

We currently believe that the error in the retrograde annual amplitude is due to an error in the resonance frequency of the "free core nutation" (FCN). The existence of this resonance which is due to the rotating, elliptical fluid core of the Earth has been confirmed by gravimetric observations. However, no observations have yet been able to confirm the value of resonance frequency which is currently calculated theoretically. We believe that our VLBI results have been able to measure both the real and imaginary components of this resonance frequency. Our estimates of the resonance frequency (computed from the corrections to the retrograde annual nutation amplitude) and the theoretical values of the resonance frequency computed for several Earth models are given in Table 1.4.4. A change in the FCN resonance frequency will introduce changes in all of the nutation series coefficients, although most of these changes will be below the current level of observability. The expected changes in the largest nutation amplitudes are shown

in Table 1.4.5. From this table we see that only the 18.6 yr nutation will change by more than 1 mas. Our three year span of data is not long enough to allow us to reliably estimate corrections to this long period nutation. However, we can study the effects of this correction on the long term behavior of the nutation angle estimates. In Figure 1.4.2 we show our residual nutation angle estimates after removing the estimated errors in the annual, semiannual and 18.6 yr terms. We see that the slope of residual corrections to the nutation in obliquity ($\Delta\epsilon$) is approximately zero -- implying that the predicted error in the 18.6 yr nutation is not contradicted by the long period behavior of our results. The residual nutation in longitude ($\Delta\psi \sin \epsilon_o$) does have a residual slope of -0.1 "/cy which could be due to an error in the precession constant. (The uncertainty of the IAU 1976 precession constant is $\pm$ 0.15 "/cy.); we, of course, can and will estimate the precession constant in future "global" analysis of VLBI data.

The scatter of our nutation angle residuals is 1.1 and 1.3 mas for $\Delta\epsilon$ and $\Delta\psi \sin \epsilon_o$, respectively. This scatter is about twice the amount we would expect from the statistics of the estimates. We are currently investigating the origin of this additional scatter which we believe to be caused mainly by diurnal atmospheric delay variations. We are also continuing our studies of the calculation of the FCN resonance frequency with the aim of determining the cause for the apparent error in the current value.

Acknowledgment

References

Carter, W.E., A.E.E. Rogers, C.C. Counselman, and I.I. Shapiro, Comparison of Geodetic and Radio Interferometric Measurements of the Haystack-Westford Base Line Vector, JGR 85, 2685-2687, 1980.

Rogers, A.E.E., C.A. Knight, H.F. Hinteregger, A.R. Whitney, C.C. Counselman, I.I. Shapiro, S.A. Gourevitch, and T.A. Clark, Geodesy by Radio Interferometry: Determination of a 1.24-km Base Line Vector with 5 mm Repeatability, JGR 83, 325-334, 1978.

Sasao, T., S. Okubo and M. Saito, A simple theory on dynamical effects of stratified fluid core upon nutational motion of the Earth, in Proc. IAU Symp. No 78, Nutation and the Earth's Rotation, Kiev, May 1977, eds. Fedorov, E.P., Smith, M.L., and Bender, P.L. 1980.

Sasao, T., and J.M. Wahr, An excitation mechanism for the free 'core nutation', Geophys. J.R. Astr. Soc. 64, 729-746, 1981.

Wahr, J.M., The forced nutations of an elliptical, rotating, elastic, and oceanless Earth, Geophys. J.R. Astr. Soc. 64, 677-703, 1981.

Table 1.2. Implied values for the error in the mapping function parameter Δa for a zenith delay of 230 cm.

Baseline*	Length (km)	Number of Samples+	$\Delta a \times 10^3$
HA-ON	5599.7	1	1.5 ± 0.4
HR-OV	1508.2	3	0.8 ± 0.3
OV-ON	7914.1	2	1.0 ± 0.2
HR-ON	7940.7	3	1.1 ± 0.1
HA-HR	3135.6	1	0.7 ± 0.2
HR-MO	1313.4	1	2.1 ± 0.3
OV-MO	245.3	1	1.6 ± 0.4
Weighted Mean			1.1 ± 0.2

* Baseline name abbreviations are as follows: HA Haystack, MA; MO Mojave, CA; HR Ft. Davis, TX; and ON Onsala, Sweden.

+ All the VLBI data listed in Section 1.2 have been used to generate this table except the data taken on the 15th and the 18th of December, 1982. These data sets are still under analysis.

Table 1.3.1 Summary of baseline lengths

Baseline	# of exps.	length[+] (m)	sigma[+] (m)	WRMS[+] (m)	NRMS[+]	WRMS[*] (m)	NRMS[*]
HA-CH	7	5,072,314.364 ± 0.006	0.029	2.16	0.028	2.28
HA-HR	30	3,135,640.956 ± 0.004	0.017	1.25	0.017	1.28
HA-OV	22	3,928,881.556 ± 0.003	0.015	1.50	0.015	1.54
HA-ON	25	5,599,714.373 ± 0.005	0.026	1.60	0.023	1.82
HA-WE	6	1239.395 ± 0.002	0.004	1.14	0.004	1.14
HA-EF	6	5,591,903.441 ± 0.006	0.024	1.53	0.026	1.74
HA-NR	3	845,129.839 ± 0.002	0.010	2.31	0.009	2.31
CH-HR	7	7,663,737.269 ± 0.010	0.060	1.88	0.063	1.98
CH-OV	7	7,846,991.133 ± 0.009	0.047	1.81	0.050	1.92
CH-ON	7	1,109,864.304 ± 0.003	0.004	0.46	0.008	1.00
CH-WE	0	5,073,265.270 ± 0.007				
CH-EF	0	589,796.542 ± 0.004				
CH-NR	0	5,834,122.784 ± 0.008				
HR-OV	26	1,508,195.356 ± 0.002	0.012	1.41	0.012	1.41
HR-ON	37	7,940,732.104 ± 0.009	0.063	1.49	0.054	1.38
HR-WE	120	3,134,927.971 ± 0.003	0.021	1.47	0.021	1.51
HR-EF	5	8,084,184.751 ± 0.011	0.064	1.54	0.043	1.05
HR-NR	4	2,354,633.977 ± 0.003	0.010	1.52	0.009	1.25
OV-ON	26	7,914,130.853 ± 0.008	0.039	1.41	0.035	1.44
OV-WE	28	3,928,579.286 ± 0.004	0.017	1.63	0.015	1.51
OV-EF	6	8,203,742.365 ± 0.010	0.049	1.99	0.048	2.00
OV-NR	4	3,324,244.142 ± 0.004	0.009	1.32	0.009	1.35
ON-WE	40	5,600,741.326 ± 0.006	0.026	1.43	0.023	1.58
ON-EF	5	832,210.499 ± 0.003	0.008	1.28	0.007	1.18
ON-NR	2	6,319,317.417 ± 0.008	0.027	1.19	0.018	0.88
WE-EF	0	5,592,850.979 ± 0.007				
WE-NR	4	844,148.075 ± 0.002	0.003	0.70	0.003	0.71
EF-NR	1	6,334,648.392 ± 0.009	0.067	2.74	0.069	2.82

Table 1.3.1 Continued.

+ 10° elevation angle cut off solution

*0° elevation angle cut off solution

The codes for the stations are: HA Haystack, Massachusetts; WE
Westford, Massachusetts; ON Onsala, Sweden; CH Chilbolton, England;
EF Effelsberg, Federal Republic of Germany; NR National Radio
Astronomy Observatory, West Virginia; HR Harvard Radio Astronomy
Telescope, Texas; OV Owens Valley Radio Observatory, California.
The repeatability of the estimates of baselines involving Westford
have been calculated including observing sessions which used the
Haystack Observatory, by inferring the lengths to Westford from
the lengths to Haystack. The speed of light used to convert measured
delays to distances was 2.99792458×10^{8} m/sec.

Table 1.3.2 Haystack-Westford baseline components[1]

Date	# of* obs.	rms+ pfr (ps)	x[#] (mm)	y[#] (mm)	z[#] (mm)	length[#] (mm)
Mark III experiments						
81/ 5/13	91	7	595.3 ± 0.5	202.3 ± 0.6	12.9 ± 1.5	395.4 ± 0.5
81/ 6/16	126	9	596.2 ± 1.0	204.0 ± 0.9	02.4 ± 2.4	396.6 ± 1.0
81/11/18	123	8	592.5 ± 0.8	203.0 ± 0.6	14.1 ± 1.6	393.1 ± 0.8
81/11/19	114	9	595.4 ± 0.7	201.9 ± 0.8	19.1 ± 2.2	395.5 ± 0.7
82/ 6/18	106	6	595.2 ± 0.7	203.8 ± 0.6	09.0 ± 1.5	395.7 ± 0.7
82/ 6/20	102	7	595.2 ± 0.6	203.6 ± 0.4	11.0 ± 1.4	395.7 ± 0.6
82/12/18	28	3	594.0 ± 0.6	204.9 ± 0.5	07.0 ± 1.4	395.1 ± 0.6
			————	————	————	————
Weighted mean			594.9	203.5	10.7	395.4
wrms scatter (mm)			1.0	1.0	4.3	0.9
			————	————	————	————
Weighted mean Mk I			594.4	201.3	4.7	394.1
wrms scatter (mm)			5.2	2.9	7.1	3.1
(Rogers et al., 1978)						
Survey results			592.	196.	24.	390.
std. deviation (mm)			2.	3.	3.	1.
(Carter et al., 1980)						

---

[1] The coordinate system is a (left-handed) Cartesian system with the x direction toward astronomic north, and the z direction along the local vertical. The astronomic latitude and longitude of Haystack used to transform our geocentric coordinate system to the local coordinate system were $42°37'21.80"$ N and $71°29'19.07"$ W, respectively (Carter et al.,1980).

*Number of observations.

+Weighted rms scatter of the postfit residuals (10 ps = 3 mm).

#The values of x,y,z, and length in these columns should be added to 1,149,000 mm, 462,000 mm, 30,000 mm, and 1,239,000 mm. The VLBI estimates of the vertical component should be corrected by +13 mm to account for a known, repeatable deformation of the Haystack antenna (Carter et al., 1980).

Table 1.4.1 Estimates of the corrections to the IAU 1976 nutation
series coefficients

| Period | $\Delta \epsilon$ | | $\Delta \psi \sin \epsilon_0$ | |
| | in phase | out of phase | in phase | out of phase |
(days)	(mas)	(mas)	(mas)	(mas)
182.6	-0.5 ± 0.2	-0.8 ± 0.2	0.7 ± 0.2	-0.3 ± 0.2
365.2	1.9 ± 0.2	-0.7 ± 0.2	1.7 ± 0.2	0.9 ± 0.2
13.7	0.0 ± 0.2	-0.1 ± 0.2	0.4 ± 0.2	0.2 ± 0.2
27.6	0.0 ± 0.2	0.1 ± 0.2	0.2 ± 0.2	-0.2 ± 0.2
121.7	0.6 ± 0.2	0.1 ± 0.2	-0.1 ± 0.2	-0.3 ± 0.2
9.1	0.0 ± 0.2	0.4 ± 0.2	-0.3 ± 0.2	-0.0 ± 0.2

The quoted standard deviations are the formal estimates multiplied by the NRMS
scatter of the nutation angle residuals. (The multiplicative factor was 2.0
for both $\Delta \epsilon$ and $\Delta \psi \sin \epsilon_0$).

Table 1.4.2 Estimates of the corrections to the
amplitudes of the
circular nutations.

| Period
(days) | Amplitude
(IAU 1976)
(mas) | Corrections | |
		in phase (mas)	out of phase (mas)
182.6 prograde	-549.1	0.6 ± 0.2	-0.6 ± 0.2
182.6 retrograde	-24.5	-0.2 ± 0.2	0.3 ± 0.2
365.3 prograde	25.7	-0.1 ± 0.2	0.1 ± 0.2
365.2 retrograde	-31.1	-1.9 ± 0.2	0.8 ± 0.2
13.7 prograde	-94.1	-0.2 ± 0.2	0.1 ± 0.2
13.7 retrograde	-3.6	0.2 ± 0.2	0.2 ± 0.2
27.6 prograde	14.5	0.1 ± 0.2	-0.0 ± 0.2
27.6 retrograde	-13.8	-0.1 ± 0.2	-0.1 ± 0.2
121.7 prograde	-21.5	-0.3 ± 0.2	0.0 ± 0.2
121.7 retrograde	-0.9	-0.3 ± 0.2	-0.3 ± 0.2
9.1 prograde	-12.5	-0.1 ± 0.2	0.2 ± 0.2
9.1 retrograde	-0.5	0.1 ± 0.2	-0.2 ± 0.2

Table 1.4.3 Effects of the ocean tides on the nutation amplitudes[*]

Period (days)			in phase (mas)	out of phase (mas)
6789.4	(18.6 yrs)	prograde	0.1	-0.1
6789.4	(18.6 yrs)	retrograde	-1.1	1.1
182.6		prograde	0.6	-0.6
365.3		retrograde	-0.2	0.2

All other amplitudes are affected at <0.1 mas.

[*] Results compiled from Wahr and Sasao (1981)

Table 1.4.4 Theoretical and estimated values of the FCN resonance frequency.

Earth model	Real component (cycles/sid. day)	Imaginary component (cycles/sid. day)
1066A Gilbert and Dziewonski[#]	-1/460.5	0
Wang (1972)[+]	-1/466.6	0
Bullen and Haddon (1967)[+]	-1/472.7	0
Guttenberg and Bullen A (1961)[+]	-1/451.9	0
VLBI estimate	-1/(432 ± 3)	-1/(20,000 ± 4,000)

[#]From Sasao and Wahr (1981)
[+]Compiled from Sasao et al. 1980.

Table 1.4.5 Estimated corrections to the nutation amplitudes due to
the change in the FCN resonance frequency

Period (days)				in phase (mas)	out of phase (mas)
6789.4	(18.6 yrs)	prograde		0.2	-0.1
6789.4	(18.6 yrs)	retrograde		-1.9	0.5
182.6		prograde		0.3	-0.1
182.6		retrograde		<0.1	<0.1
365.3		prograde		<0.1	<0.1
365.3		retrograde		-2.1	1.0

Figure 1.1.1. Group delay closures for 3C345 for the
Haystack-Effelsberg-Onsala baseline triplet, from an experiment
beginning on 28 August 1980. The solid line is an estimate of the
feed polarization error.
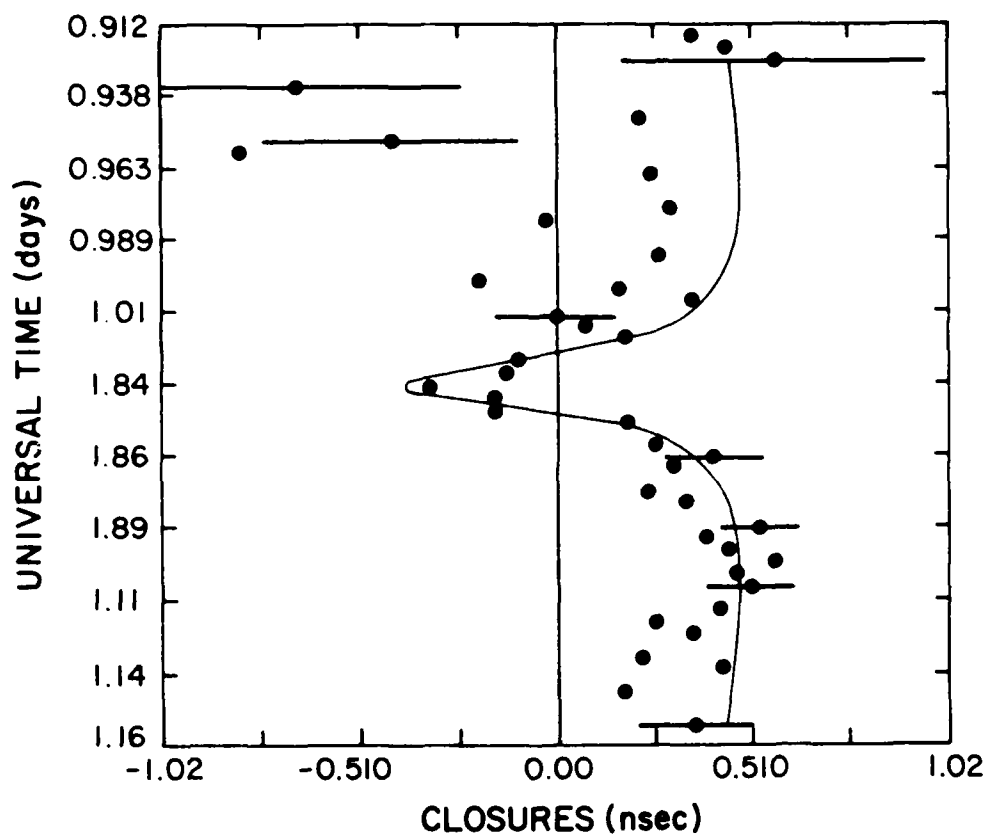
Figure 1.1.2. The effects of the feed polarization error on the implied S-band group delay measurements, from an experiment beginning on 18 December 1982. Data from the Ft. Davis to Owens Valley baseline are shown. The dashed line is an estimate of the feed polarization error.

IMPLIED S-BAND GROUP DELAY ERRORS (nsec)
(based on group delay predictions from phase
connected phase delays)
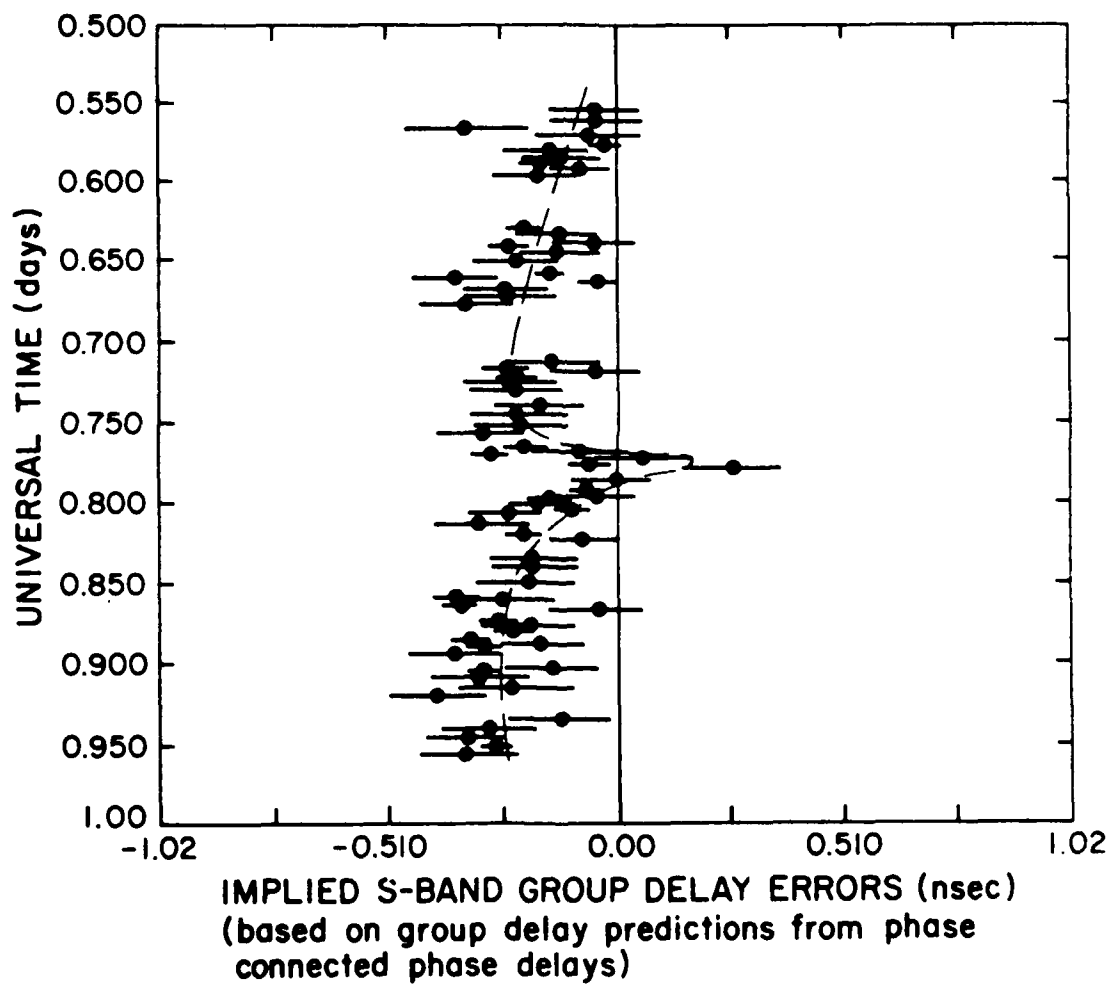
Figure 1.2. Differences between baseline length estimates from solutions with and without zenith delay corrections estimated.

Slope = (1.1 ± 0.2) × 10⁻³ cm/km

(constrained to pass through origin: see text)
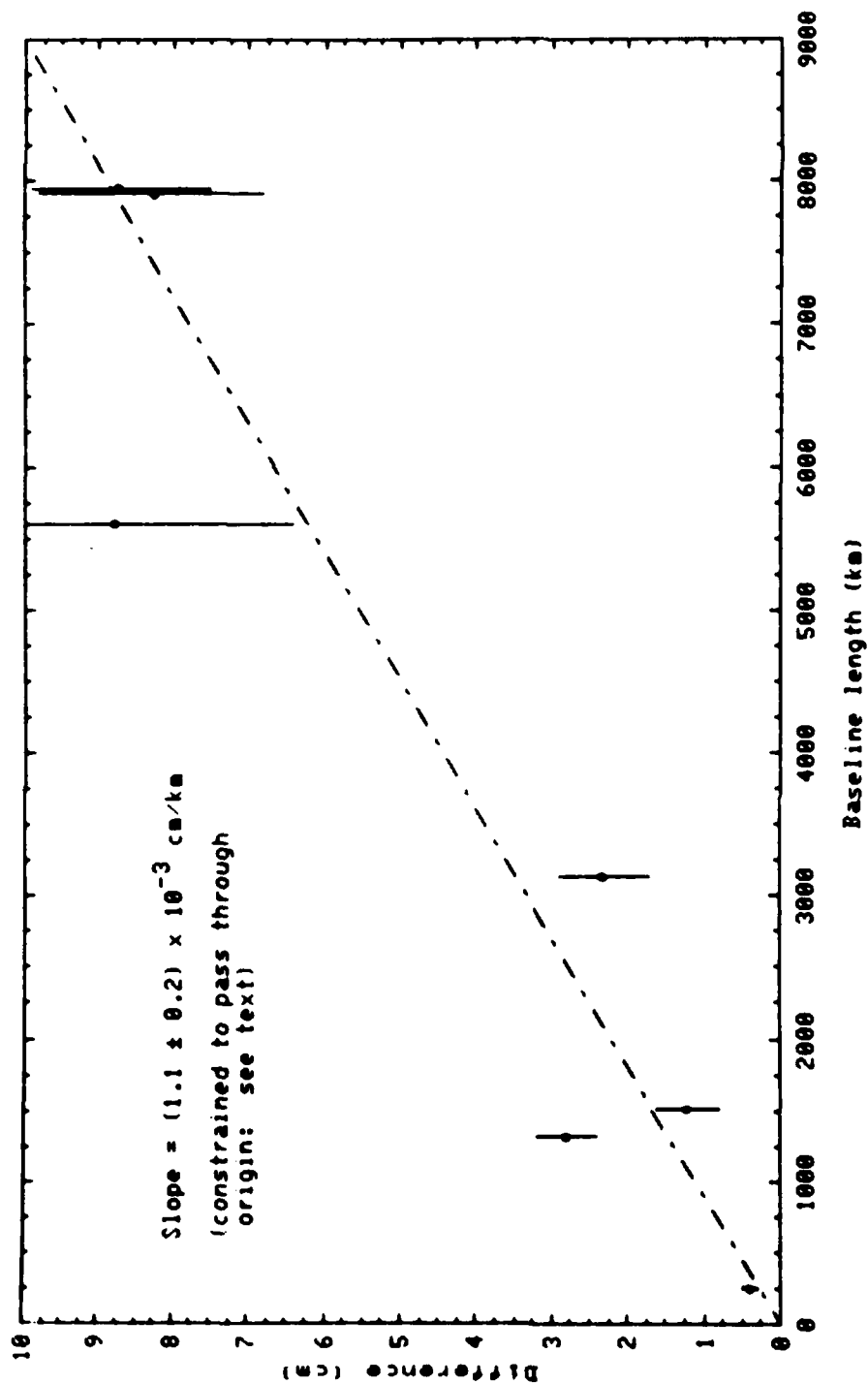
Figure 1.3.1 Changes of baseline length with changes of the
elevation angle cutoff.

a.

0° elevation cut-off solution - 10° elevation cut-off solution

b.

10° elevation cut-off solution - 15° elevation cut-off solution

Figure 1.3.1 continued.

c.

6.0   10° elevation cut-off solution – 20° elevation cut-off solution

Difference (cm)
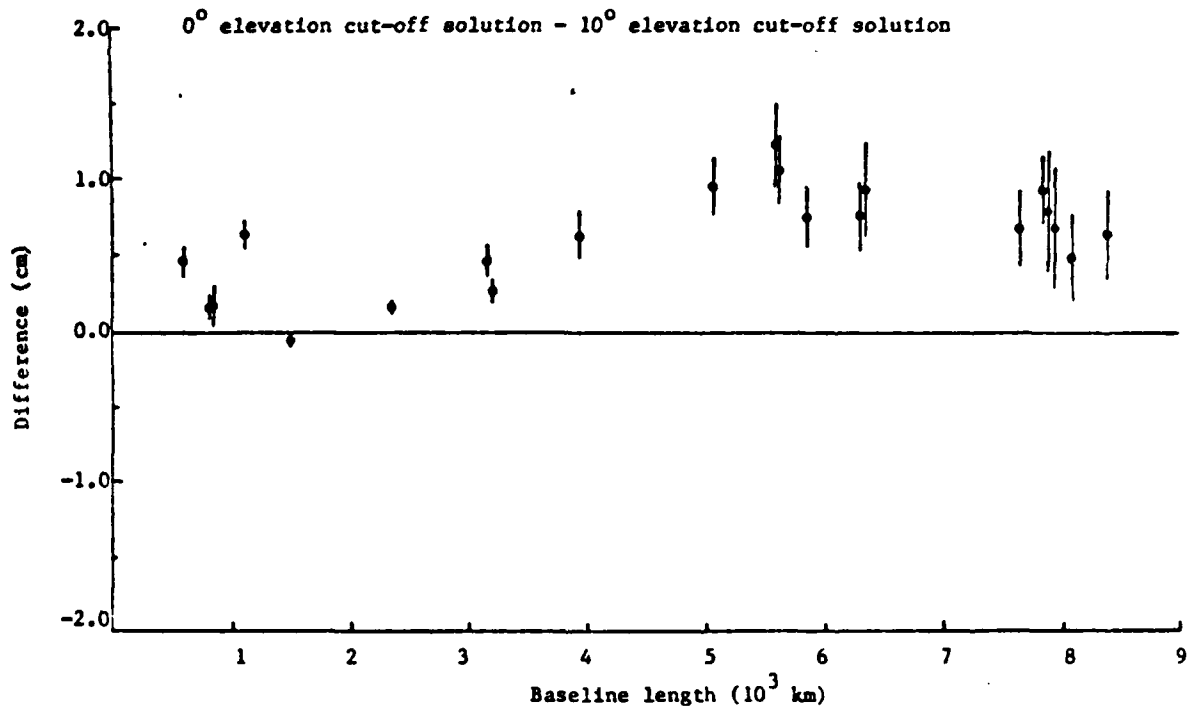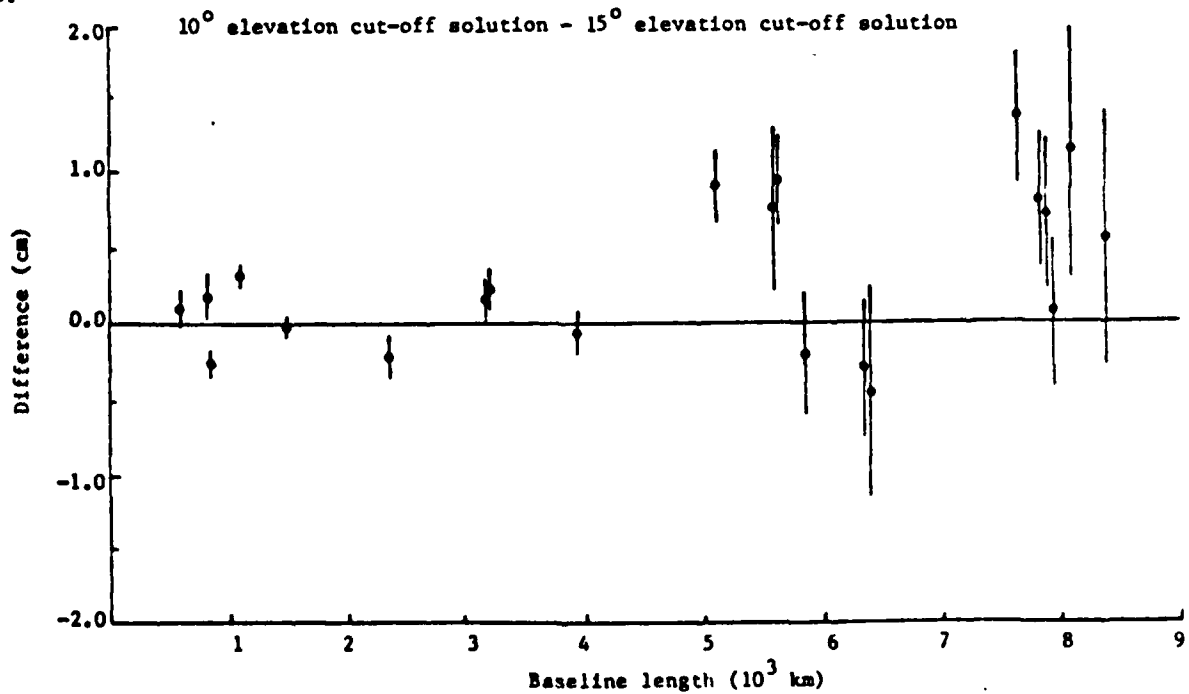
Baseline length (10³ km)
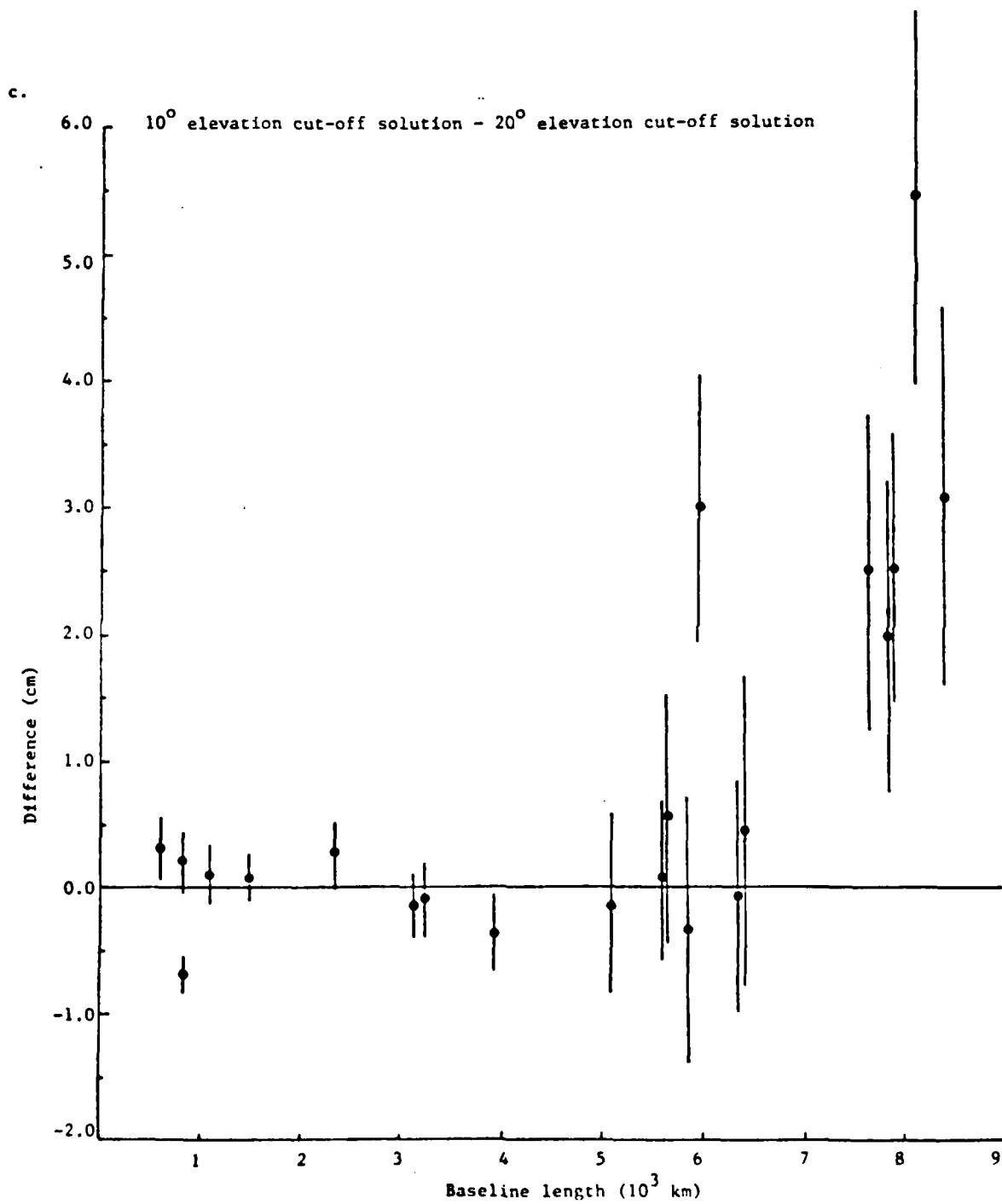
Figure 1.3.2   The effects of changing the atmospheric delay calibration.

10° elevation cut-off solution with surface weather model for the atmospheric delay minus
10° elevation cut-off solution with no surface weather model
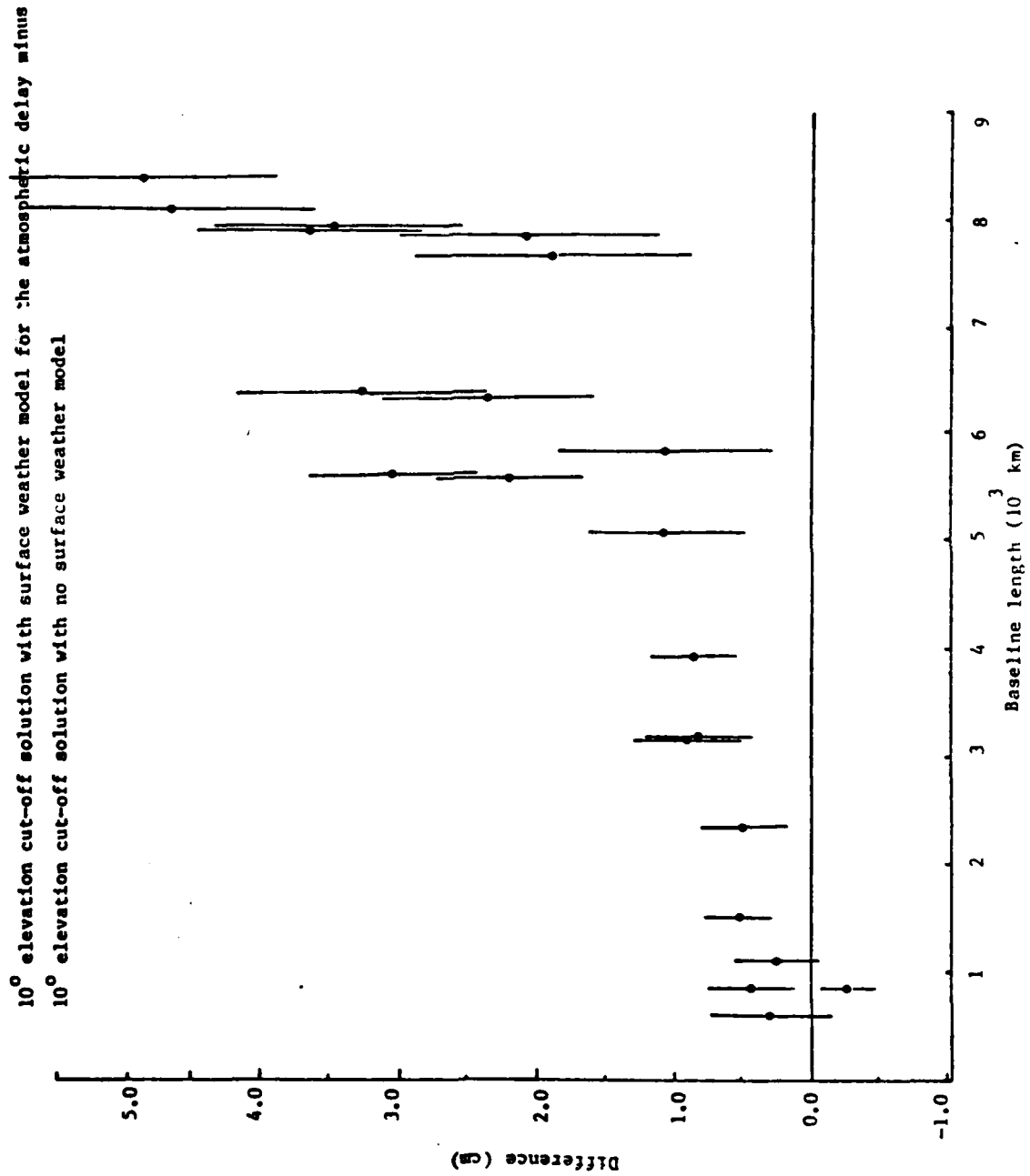
Figure 1.3.3   Westford to Onsala baseline length estimates from the 10° elevation
angle cutoff solution.

WRMS scatter about the mean   2.5 cm
WRMS scatter about the slope 2.0 cm

Slope 1.6 ± 0.5 cm/yr

Differences from Baseline, cm

8.0
6.0
4.0
2.0
0.0
-2.0
-4.0
-6.0
-8.0
-10.0

Jul
1980

Jan
1981

Jul

Jan
1982

Jul

Jan
1983

Jul
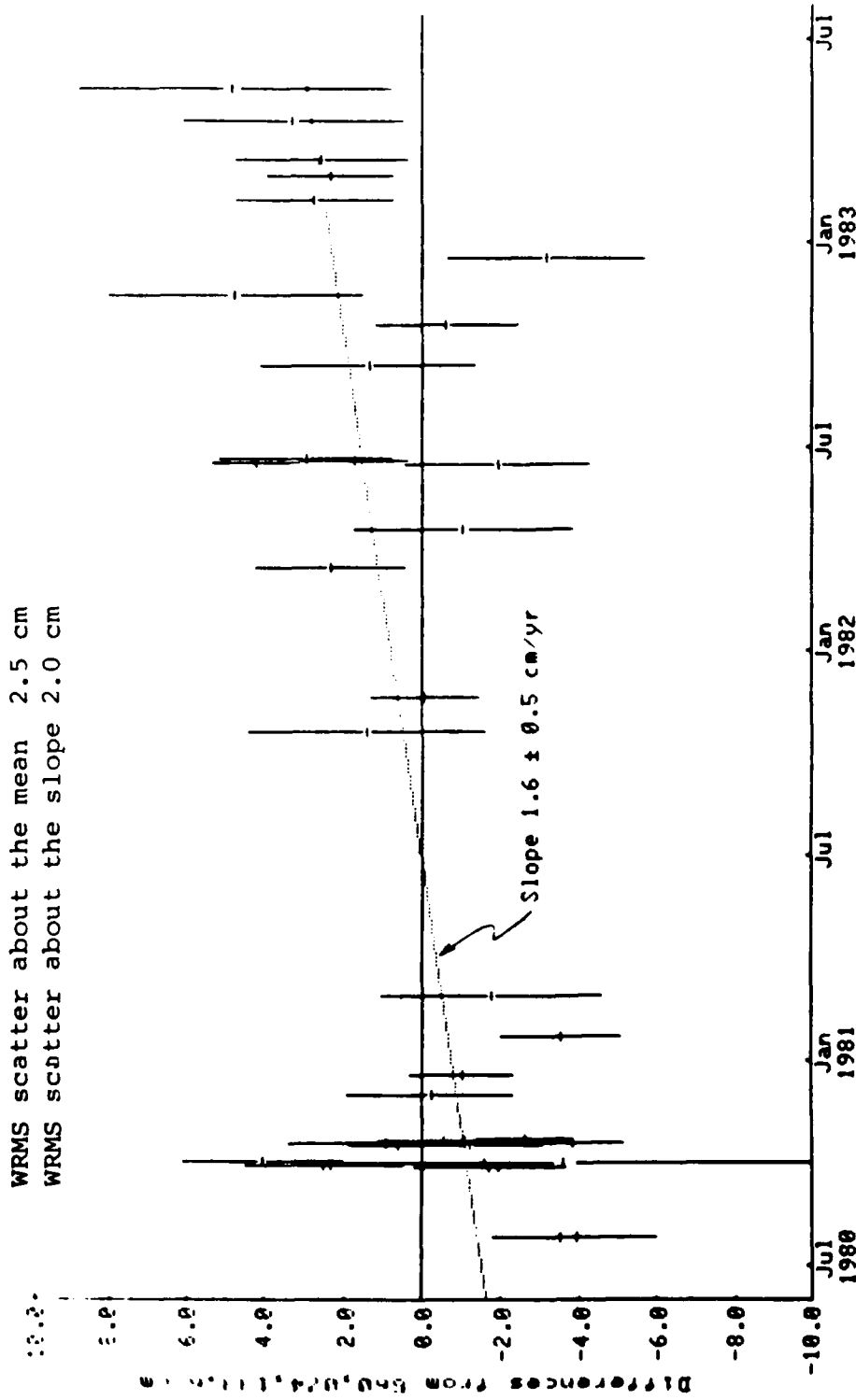
Figure 1.3.4.a The Westford antenna horizontal coordinates

points
1   81/5/13
2   81/6/16
3   81/11/18
4   81/11/19
5   82/6/18
6   82/6/20
7   82/12/18
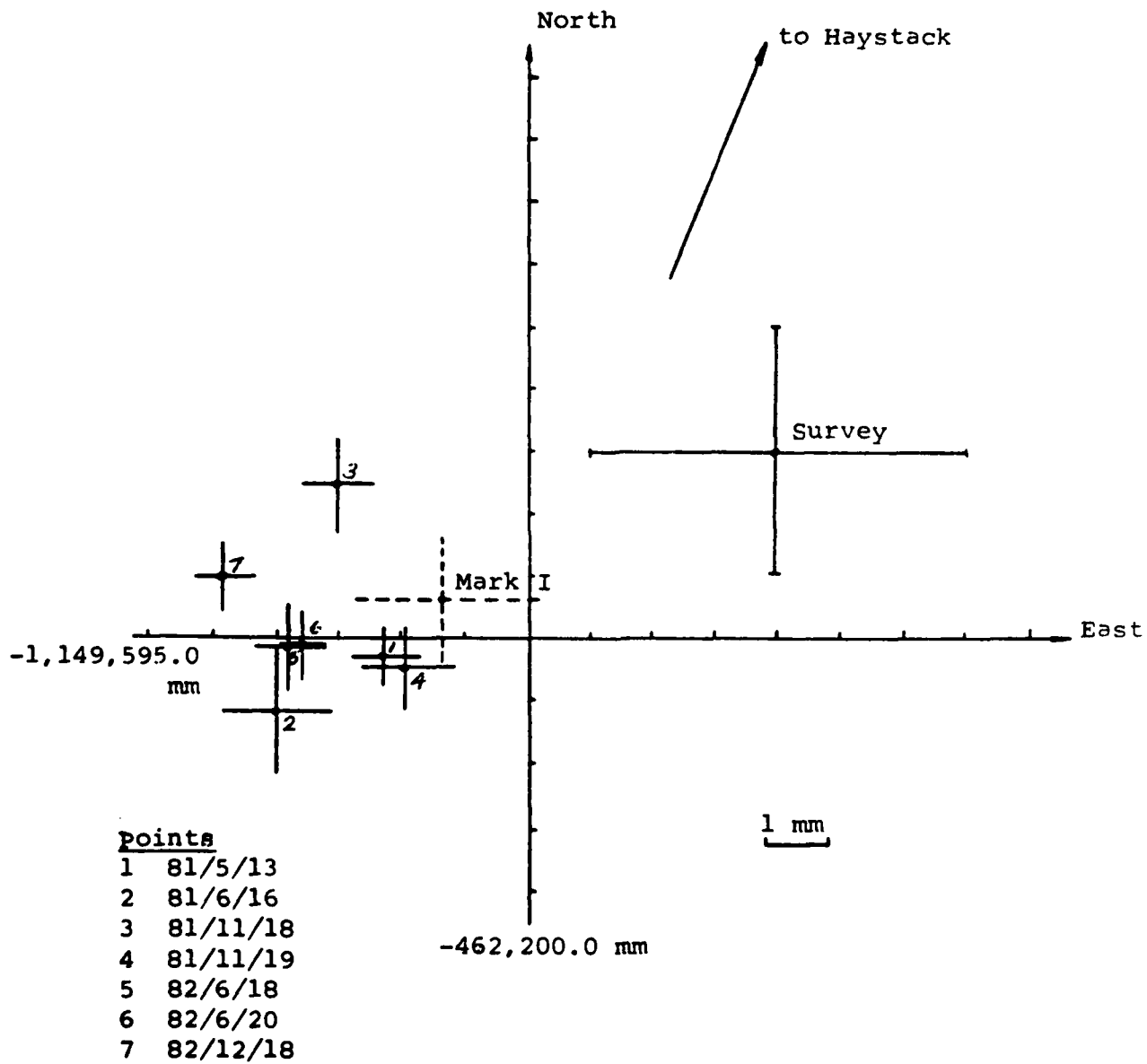
Figure 1.3.4.b Westford vertical coordinate verus Haystack-
Westford baseline length.
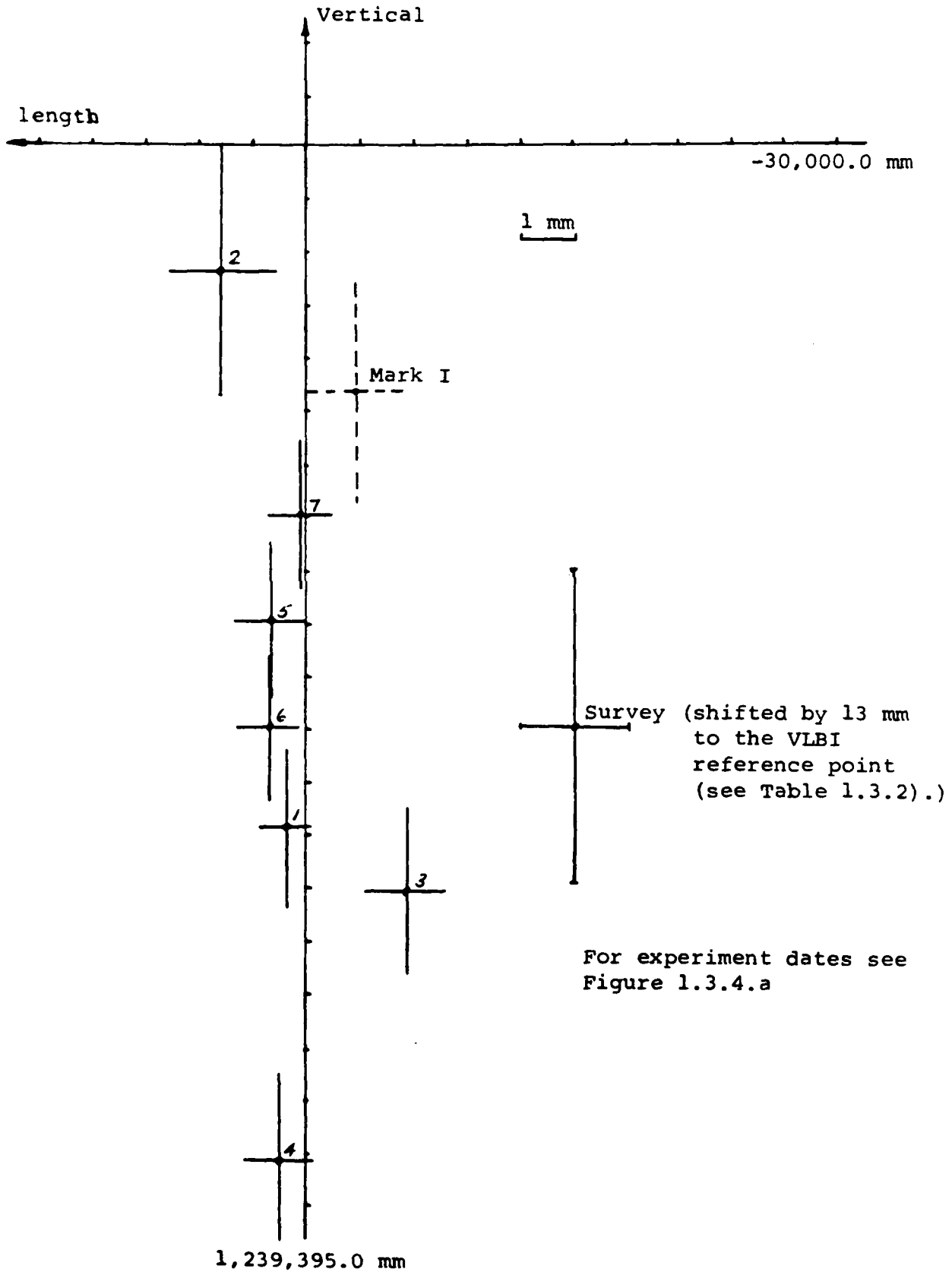
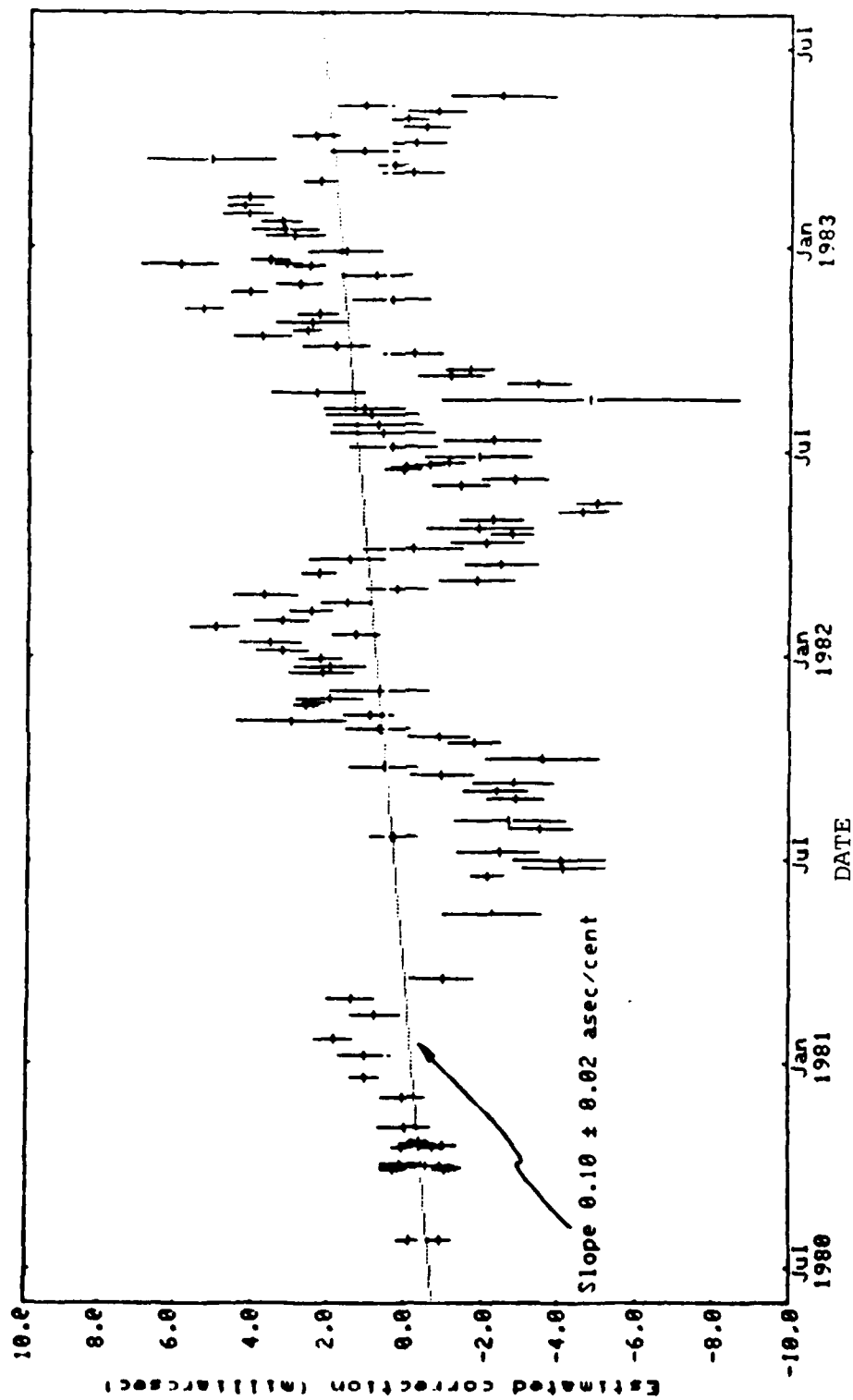Figure 1.4.1.a Estimated corrections to the nutation in obliquity Δε.

Figure 1.4.1.b Estimated corrections to the nutation in longitude $\Delta\psi\sin\epsilon_0$.
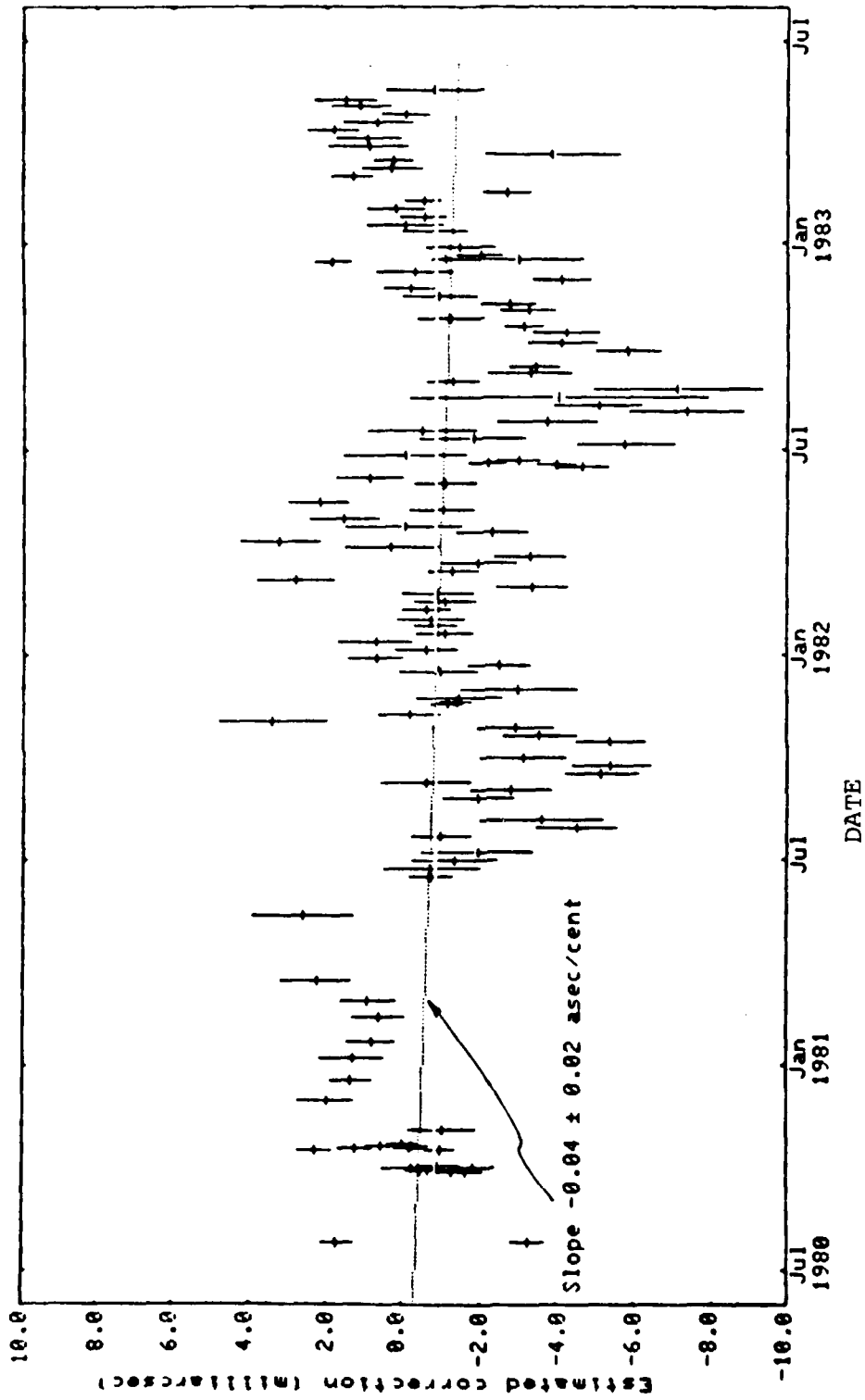
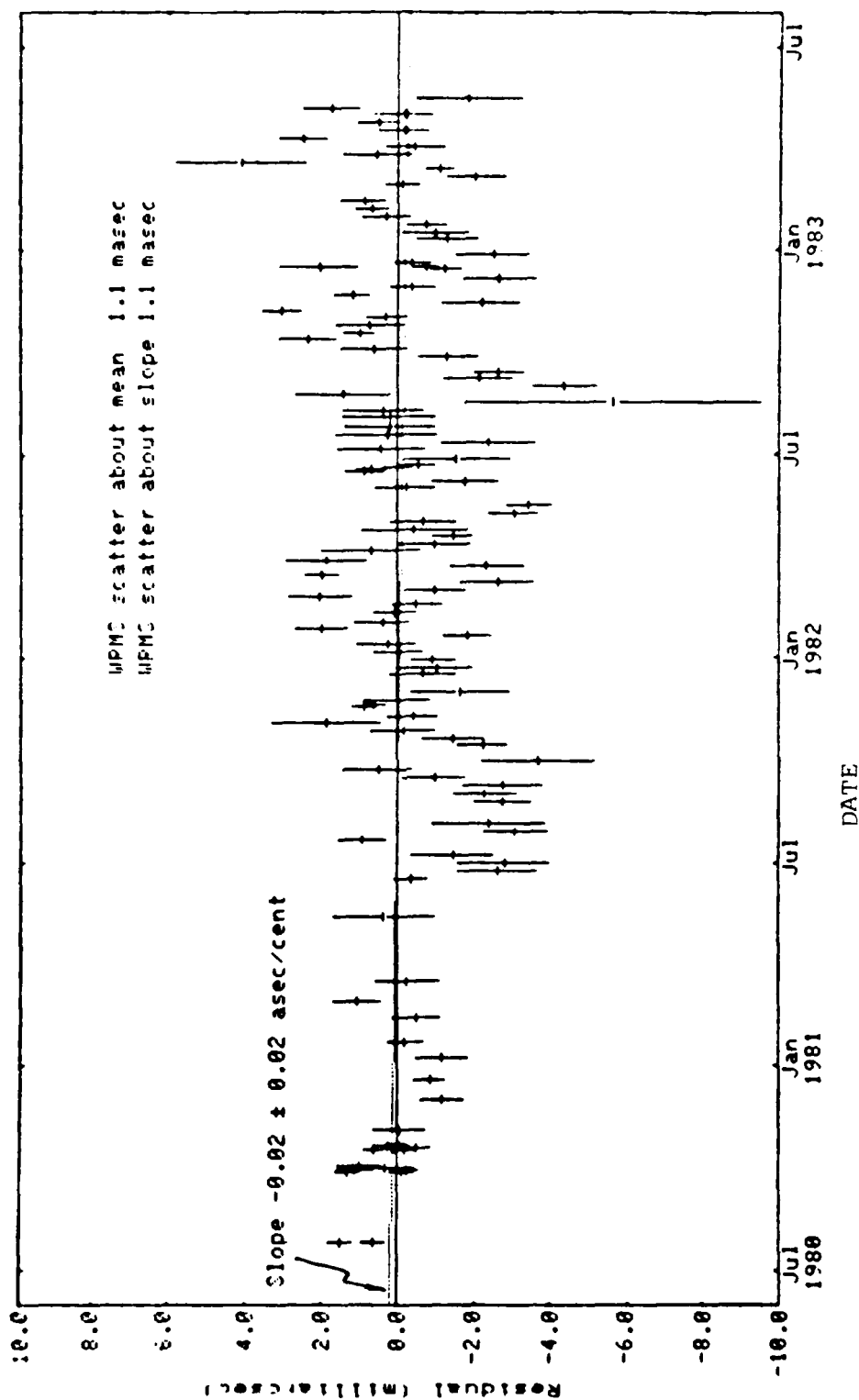Figure 1.4.2.a   Residual corrections to the nutation in obliquity.

Figure 1.4.2.b Residual correction to the nutation in longitude.